Fuel 105 (2013) 523–534

Contents lists available at SciVerse ScienceDirect

Fuel

journal homepage: www.elsevier.com/locate/fuel

A comparative experimental study of the interactions between platinum and a range of hydrocarbon fuels

J. Badra [a,*], A.R. Masri [a], C. Zhou [b], B.S. Haynes [b]

[a] School of Aerospace, Mechanical and Mechatronic Engineering, The University of Sydney, NSW 2006, Australia
[b] School of Chemical and Biomolecular Engineering, The University of Sydney, NSW 2006, Australia

HIGHLIGHTS

- The reactivity of four different alkanes ranging from C_1 to C_4 is tested over platinum.
- The platinum plate temperature peaks at moderately rich ethane/air mixtures.
- The reactivity limits of ethane/air mixtures broaden in the presence of platinum.
- Compressed natural gas show higher selectivity towards CO and H_2.
- Two distinct reactive zones are observed in the streamwise and transverse directions.

ARTICLE INFO

Article history:
Received 19 June 2012
Received in revised form 10 August 2012
Accepted 13 August 2012
Available online 29 August 2012

Keywords:
Catalytic combustion
Reactivity limits
Homogeneous and heterogenous reactions
Micro-combustion

ABSTRACT

This paper presents the reactivity of different alkanes ranging from C_1 to C_4 over platinum. The four fuels used are compressed natural gas (CNG), liquefied petroleum gas (LPG), butane, and ethane. Experiments are performed to study the effects of varying the temperature of the incoming mixture (T_{jet}), its equivalence ratio (φ) and the Reynolds number (Re), on the reactivity limits and species distributions. Platinum surface temperatures as well as species profiles streamwise and transverse to the plate are investigated. The reactivity limits of ethane over platinum are discussed in details.

For flameless combustion (defined by the the presence of reactions on the plate without a gaseous flame), it is found that the plate temperatures of ethane/air peak at moderately rich mixtures ($\varphi = 1.3$) and the reactivity limits broaden in the presence of platinum plate compared to the gaseous flammability limits. The main products of burning these four hydrocarbon fuels over platinum are CO_2 and H_2O while CNG showing the highest selectivity to CO and H_2. Species such as methane (CH_4), acetylene (C_2H_2), ethane (C_2H_6), dimethyl ether (C_2H_6O), propylene (C_3H_6), and propane (C_3H_8) appear in the products when burning LPG and butane over platinum. The streamwise profiles of species indicate the presence of two reacting zones along the plate which are described as: (i) the leading edge zone where high gradients of species mole fractions are observed and (ii) the trailing zone where the profiles are more flat and stable. The transverse profiles highlight the presence of two reactive layers: (i) the inner boundary where peaks of CO, CO_2, and H_2 occur and (ii) the outer layer where formation of the other hydrocarbons is observed. Heavier alkanes result in oxygen/fuel ratio near the plate higher than those injected in the free stream and this may be largely due to differential molecular as well as thermal diffusion.

1. Introduction

A thorough understanding of the interactions between gaseous and surface chemistries is a necessary prerequisite for the development of stable and efficient micro-combustors that may be used in micro-power generation [1–4] or in the replacement of batteries in portable electronic devices [1,5]. Such knowledge would also be extremely useful in fuel processing technologies where the range of working temperatures is lower [6–9]. While the fuels and catalysts used vary depending on the application, the key difficulties are common in that the fluid–solid interface involves a complex exchange of homo–heterogeneous reactions and heat management is vital considering the large surface to volume ratios that dominate micro-reactors.

It is convenient here to classify micro-reactors nominally in two broad categories: flaming and non-flaming. Flaming micro-combustors involve the stabilization of either a premixed [10–12] or

* Corresponding author. Tel.: +966546612705; fax: +61 2 9351 3760.
E-mail addresses: jihad.badra@sydney.edu.au (J. Badra), assaad.masri@sydney.edu.au (A.R. Masri), ryan.zhou@sydney.edu.au (C. Zhou), brian.haynes@sydney.edu.au (B.S. Haynes).

0016-2361/$ - see front matter © 2012 Elsevier Ltd. All rights reserved.
http://dx.doi.org/10.1016/j.fuel.2012.08.021

diffusion flames [1,13,14] and operate at relatively high temperatures leading to significant heat losses and issues with flame stability. In the case of diffusion flames, mixing fuel and oxidant is a challenge that requires special configurations for the fluid streams considering that the flow is laminar and mixing rates are controlled mainly by molecular diffusion [1,13,15]. Non-flaming micro-reactors generally make use of catalytic surfaces and operate in lower temperature ranges as dictated by the process and the catalyst. The focus of this paper is on the latter category using platinum with a range of gaseous hydrocarbon fuels.

Earlier research on non-flaming micro-combustors has studied a range of flow geometries [15] such as stagnation flow [16], axisymmetric tube [17,18], rectangular channels [14], and flat unconfined plate [19,20], but remains limited to fuels such as hydrogen, carbon monoxide, methane and propane. Channel flows sandwiched between two parallel catalytic plates were studied using propane [21–23], hydrogen [11,16,24], methane [25–27] as well as CO–H_2/air mixtures [28]. In Stefanidis and Vlachos [23] the bulk inlet velocity of the (lean) fuel/air mixture was varied as well as the separation between the plates and their conductivities. It was concluded that while low inlet velocities favor surface reactions, homogeneous gas chemistry continued to play a role, albeit decreasing, with decreasing gap size, to separations as low as 200 μm. The stability limits for methane were found to be wider than propane and this was attributed to the Lewis number effects which enhance "transverse transport towards the catalytic surface".

Mantzaras and his group [21] performed detailed laser diagnostics measurements of species concentrations using LIF-Raman scattering confirming their calculations and showing that the reactor stability improves at higher pressure [21]. Also, Heatwole et al. [29] conducted experiments with lean methane/air mixtures and used an FTIR-based spectroscopic technique that exploits silicon's transmissivity in the infrared to make nonintrusive measurements of species concentration and temperature profiles in micro-combustors. Volchko et al. [30] studied the reactivity of methane/air mixtures with equivalence ratios that are richer than the flammability limits obtained in platinum micro-tubes. They showed that catalytic reactions could support combustion in mixtures even when gas-phase chemistry does not play a significant role. Also, Spadaccini et al. [31] fabricated a three-wafer catalytic combustor for a micro-scale gas turbine engine and reported efficiencies in excess of 40% for ethylene/air and propane/air combustion.

Maruta [32] have investigated the stability limits of methane/air mixtures within a Swiss roll micro-reactor. Ahn et al. [33] have found that using the same configuration (Swiss roll), the reactive limits of propane over platinum are broad and cover the equivalence ratio range of 0.2–40 [33]. This broadening has been attributed to the reactivity of propane/air mixtures over platinum, especially the enhancement of O_2 desorption at low Reynolds numbers [33]. Smyth et al. [19] have used methane to study its interaction with platinum on a simple configuration of a flat plate positioned in a co-flowing premixed fuel/air mixture. They measured temperature as well as selected species sampled from the plate's proximity and concluded that the reactive layer along the plate can be nominally split into three zones [19]. Zone I is very close to the leading edge where sharp temperature increases are noted accompanied by fast depletion of the gaseous reactants. Zone II is towards the middle where the surface temperatures plateau at a high value and reactant concentrations remain low. Zone III is towards the trailing edge where extinction of the non-adiabatic reaction is experienced and a replenishment of reactants from the free stream was observed. More recently, Smyth and Kyritsis used the same set-up but with the propane fuel to report novel flow-field as well as composition measurements in the vicinity of the plate [20].

This study adopts a flow configuration similar to that reported in Smyth et al. [19]. In an earlier paper [34], compressed natural gas (CNG), liquefied petroleum gas (LPG), commercial butane and dimethyl ether (DME) reacting on a platinum surface were studied over a range of equivalence ratios, temperatures and velocities. Measured surface temperatures were reported for all four fuels but numerical calculations, using detailed surface and gas chemistries were performed for methane only. It was concluded that: (i) the reactive limits of all fuels studied here on platinum are much broader than those of the gas-phase alone, (ii) the surface chemistry is largely controlling the heat and species release and (iii) the plate surface temperature peaks at moderately rich mixtures for all fuels except CNG where it peaks at stoichiometry. This paper extends the study to include detailed measurements of species sampled at varying distances from the plate. Additional results are reported and compared for the following fuels: compressed natural gas (CNG), ethane, liquefied petroleum gas (LPG), and butane.

2. Experimental set up

The configuration adopted here uses a premixed fuel/air mixtures co-flowing around a flat vertical unconfined platinum plate. Four hydrocarbon fuels with increasing carbon content from C_1 to C_4 are studied here. A schematic of the experimental apparatus is shown in Fig. 1 and more details may be found in [34]. The 30 cm long heater (TEMPCO) consists of a ceramic shell containing a heating coil with a diameter of 8 cm surrounding a 24 mm-OD and 23 mm-ID stainless steel tube. The fuel/air mixture flows over baffle plates positioned inside the stainless steel tube to increase the heat transfer and achieve exit temperatures up to 600 °C for Reynolds numbers based on the jet exit diameter ranging from 250 to 1500 and with equivalence ratios that range from $\varphi = 0$ to $\varphi = \infty$. The Reynolds number Re_d is calculated at the jet exit temperature (T_{jet}) and since the choice of the reference length scale is arbitrary so the corresponding approach velocities are also provided for convenience. An arrangement of meshes is used within the tube and a sintered bronze plate is placed at the exit plane to keep the flow exiting the tube laminar ($Re_d < 2000$) and uniform in both temperature and velocity. Gas issuing from the 23 mm-ID stainless steel tube flows over both sides of the platinum plate, which has a width of 6 mm, length of 20 mm and a thickness of 0.25 mm. The platinum plate is held by two pointy ceramic pins as shown in Inset A of Fig. 1. It should be noted that the ceramic was machined to minimize the area of contact with the platinum plate so that the heat losses are negligible.

This region over which flow from the tube extends without being affected by the laboratory air is referred to here as the "valid region". It is important that the entire platinum plate remains in this "valid region" surrounded by the mixture being studied and not be subjected to laboratory air. To ensure this, it was found from an earlier study that a Reynolds number of more than 200 should be used. All measurements reported here ensured that the platinum plate is fully engulfed by the mixture issuing from the jet so that the results are neither dependent on the separation from the leading edge of the nozzle nor on the nozzle diameter. A PID controller (Novus N1200) is used to regulate the temperature of the mixture at the exit plane of the burner which is measured using a type-K thermocouple. The temperature of the gases exiting the tube can be varied within the range from ambient up to 600 °C. Tylan and Bronkhorst mass flow controllers are used to control the flow rates of fuels and air, respectively.

Four different fuels, namely compressed natural gas, liquefied petroleum gas, butane, and ethane have been tested over platinum at various conditions. The parameters varied during the experiments are (i) the equivalence ratio, φ of the fuel mixture co-flowing over the platinum, (ii) its temperature at the jet exit plane, T_{jet}, and

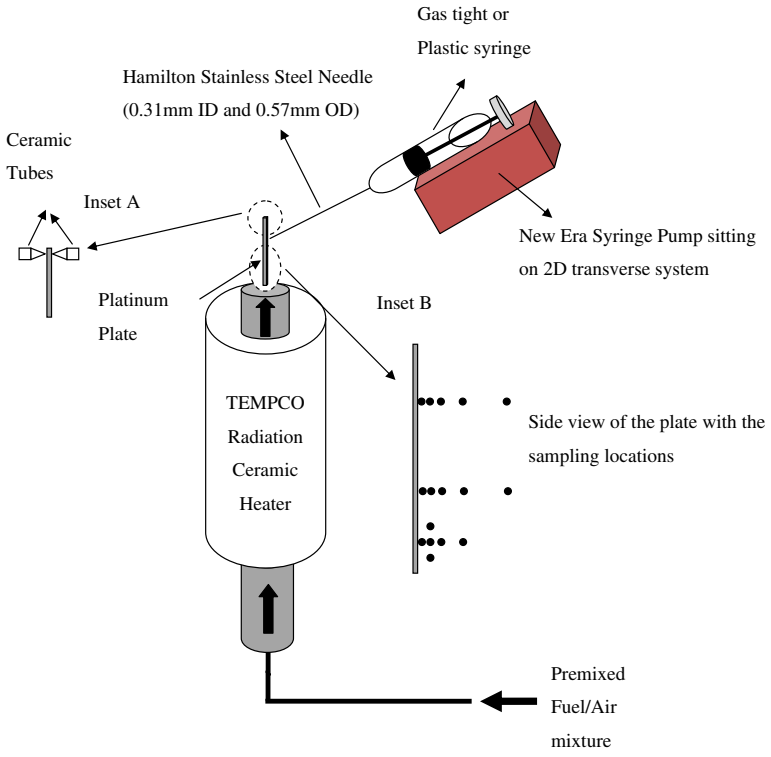

Fig. 1. Gas sampling experimental set up showing the contact mechanism between the platinum plate and the ceramic holders as well as a 2D view of the sampling experimental locations.

Table 1
Details of the volumetric fuel compositions and the experimental conditions covered in this study.

Fuel	Volumetric fuel composition
CNG	88.8% CH_4, 7.8% C_2H_4, 1.9% CO_2 and 1.2% N_2 with the remaining 0.3% being a mixture of propane, propene, butane and pentane
LPG	95% C_3H_8, 4% C_4H_{10}, 1% C_5 + hydrocarbons
Butane	99.95% C_4H_{10} and 0.05% CO_2
Ethane	99% Ethane

(iii) its Reynolds number Re_d which is based on the 23 mm-ID of the fuel tube. The composition of CNG, LPG, butane, and ethane as obtained from the supplier are presented in Table 1. The surface temperature of the platinum was measured using a two-color infrared pyrometer (Mikron M90R) that covers a range between 700 °C and 2000 °C. The emissivity of the platinum is assumed to be wavelength independent and an emissivity ratio of 1 is used throughout the measurements. The detection bands of the instrument are around 0.9 μm to avoid the infrared transmittance of major combustion products. For surface temperatures below 700 °C, an estimate is obtained by using a type-K thermocouple to measure the gas temperature just downstream the platinum plate.

Once steady state is established for a particular flow condition, and if the fuel/air mixture does not self-ignite on the platinum surface, ignition is induced using a blow torch. If a gaseous flame is maintained immediately after ignition then the flame is forced to blow off. Subsequent to this, one of the following scenarios may then prevail:

- *Extinction*: The platinum plate cannot sustain reaction and its temperature stabilizes at that of the co-flowing mixture.
- *Flaming combustion*: Subsequent to the initial ignition and blow-off, a flame re-ignites, propagates back and stabilizes on the exit plane of the fuel tube. No measurements are made with this mode of combustion since the plate is shrouded with hot combustion products.
- *Flameless combustion*: No flame is re-ignited subsequent to the initial blow-off but the platinum plate remains re-active. While in some cases the plate may be clearly red-hot, this does not have to be the case since surface reactions may be maintained at much lower temperatures as will be evident from the results presented here.

2.1. Gas sampling methodology

Gas sampling at the plate is performed for a range of cases selected for each of the four fuels studied here. Gas samples are extracted from 16 different locations along the streamwise and transverse directions of the platinum plate as shown in Inset B of Fig. 1. At 200 μm away from the plate, 5 data points are used for measurements in the streamwise direction and are located 1 mm, 2 mm, 3 mm, 5 mm, and 10 mm from the leading edge. This forms the streamwise profile of the species along the plate. The transverse profiles are taken at 2 mm, 5 mm, and 10 mm. There are 4 data points at 2 mm located 0 mm, 0.2 mm, 0.5 mm, and 1 mm away from the plate and 5 data points at 5 mm and 10 mm located 0 mm, 0.2 mm, 0.5 mm, 1 mm, and 1.8 mm away from the plate. All of the measurements are taken along the middle of the platinum plate. For each case, a sample of unreacted mixture is taken from the jet exit plane and analyzed.

A NewEra single syringe pump NE-1010 is used to control the suction and injection flow rates and the volume that needs to be withdrawn or infused. Monoject 140 ml plastic syringes, made by Covidien, and 50 ml gas tight syringes, made by SGE, are used as the sampling carriers. The syringes are placed on the pump with SGE valves attached to the tips and a Hamilton stainless steel needle (5 cm long, 0.31 mm-ID, and 0.57 mm-OD) connected to the valve. The needle is positioned near the platinum plate with the

aid of a magnifying lens. Using a controlled suction rate of 4 ml/min, a sample of 40 ml is withdrawn. It should be noted here that several tests were performed over a range of suction rates and 4 ml/min was subsequently selected as the most suitable in minimizing disturbance to the flow. The velocity within the needle is estimated at about 1 m/s which is close to the velocity of the flow in the vicinity of the plate. The gas samples are now ready for analysis which occurs within a maximum of 2 h from sample collection. Both gas tight and normal plastic syringes were tested for leakage and it was confirmed that, within the time span of the sample collection and analysis, the leakage rates from both types of syringes are negligible. Therefore, no distinction is further made between the gas tight and plastic syringes.

2.2. Gas analysis methodology

Before entering the GC, the gas samples must pass through a Perma Pure Dryer to remove all liquid water and water vapor. The gas sample exiting the Perma Pure Dryer is then delivered to a micro Gas Chromatogram (GC) (Varian CP-4900) where the concentrations of CH_4, C_2H_2, C_2H_6, C_2H_6O (DME), C_3H_6, C_3H_8, C_4H_{10}, O_2, CO_2, CO, H_2, and He will be determined. The micro GC is equipped with two independent analysis modules. Each module extracts a small amount of the sample flow using separate internal sample pumps. CH_4, C_2H_2, C_2H_6, C_2H_6O (DME), C_3H_6, C_3H_8, C_4H_{10}, and CO_2 can be analyzed directly on an 8 m PoraPlot Q (PPQ) low temperature column. Though H_2O, one of the major products, is also detectable on this column, it is impossible to gain reliable measurements due to the asymmetric peak obtained. Some species, such as C_4H_{10} and C_2H_6O (DME), require a specific set of conditions for the column referred to as PPQ (high temperature). The measurements of O_2, CH_4, CO, H_2, and He are achieved on a 10 m Molecular Sieve 5A (MS-5A) column.

The GC is calibrated by using special gas calibration cylinders with known concentrations of the gases. The mixture is fed to the GC and the signal is recorded. Then the mixture is diluted with nitrogen, fed to the GC again, and the signal is recorded. This is repeated over a sufficient number of dilution ratios to enable a calibration curve to be fitted for each species of interest. Based on the average absolute discrepancy obtained in the calibration, as well as the uncertainty of the gas composition in the cylinder (2%), mass flow controllers (2%), and micro GC (2%), a relative error of less than 6% is estimated for the measurements of CH_4, C_2H_2, C_2H_6, C_3H_6, C_3H_8, C_2H_6O (DME), C_4H_{10}, O_2, CO_2, CO, H_2, and He.

The procedure to correct for water removal from the sample and recovering the wet-based mole fractions requires the presence of an inert tracer in the sample. In addition to nitrogen, a second inert tracer was introduced by adding approximately 5% by volume of helium to the premixed fuel/air mixture. The following procedure is then followed in the analysis:

- Three conversion factors, F_i were generated using nitrogen, helium or carbon element, respectively as conserved scalars. These are obtained from the ratio of the number of moles in the products, $n_{i,P}$ and reactants, $n_{i,R}$ as follows: for helium ($F_{He} = n_{He,P}/n_{He,R}$), nitrogen ($F_{N2} = n_{N2,P}/n_{N2,R}$) and carbon ($F_C = \Sigma n_{C,P}/\Sigma n_{C,R}$).
- The measured number of moles for all species was corrected by one of these factors and the number of moles of water is then deduced by performing an atomic balance for hydrogen (H). New wet-based mole fractions, based on total number of moles are then obtained.

Several tests were performed using the three different conversion factors, and it was found that F_{N2} based on nitrogen is the most reliable. This is because significant molecular and thermal diffusion of helium was introducing bias in F_{He} and potential carbon loss due to soot precursors may be affecting F_C particularly for rich samples. Therefore wet-based results reported in this paper use the conversion factor obtained from nitrogen as the inert tracer where the value of F_{N2} used ranged from 1.03 to 1.2 depending on the fuel, case, and sampling location. The maximum experimental error in the measured number of moles of oxygen, carbon, and hydrogen to carbon (H/C) ratio is of the order of 15%. It is expected here that, while not possible to quantify experimentally, differential molecular diffusion as well as thermal diffusion are major contributor to this error.

3. Results and discussion

The findings are presented in three sections. First, the measured peak surface temperatures and reactivity limits for ethane are documented to complement earlier measurements for CNG, LPG, DME, and butane [34]. The species mole fractions (presented on a wet-basis) and temperature profiles measured at various locations

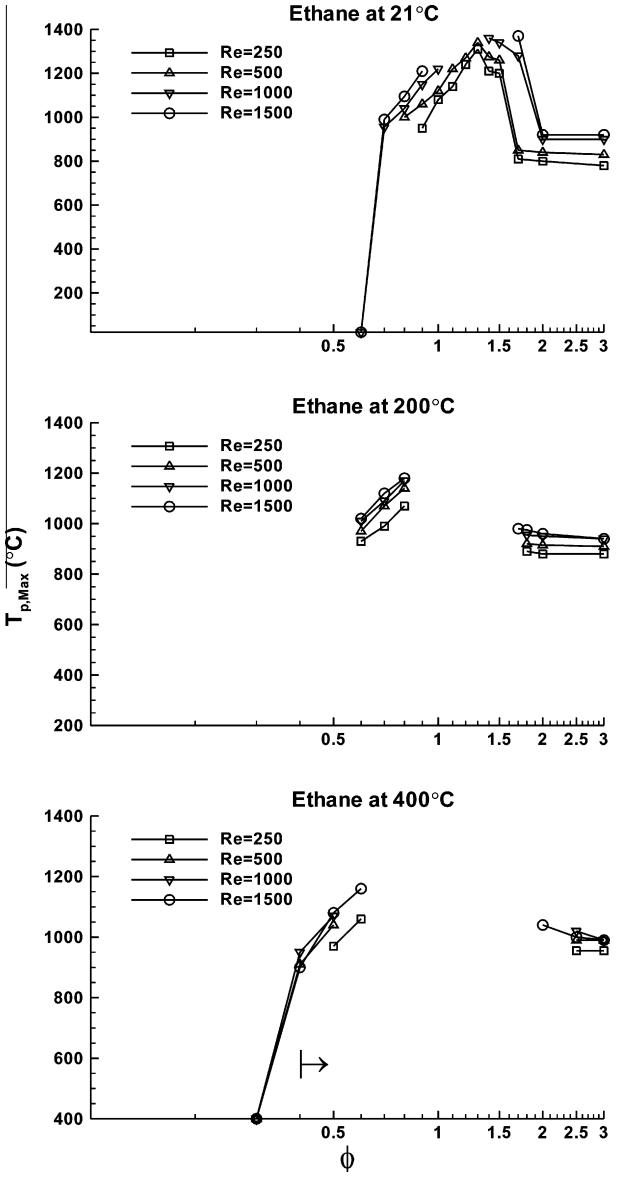

Fig. 2. Maximum measured surface temperature plotted vs. equivalence ratio φ (on a logarithmic scale) for ethane at different values of T_{jet} and Re.

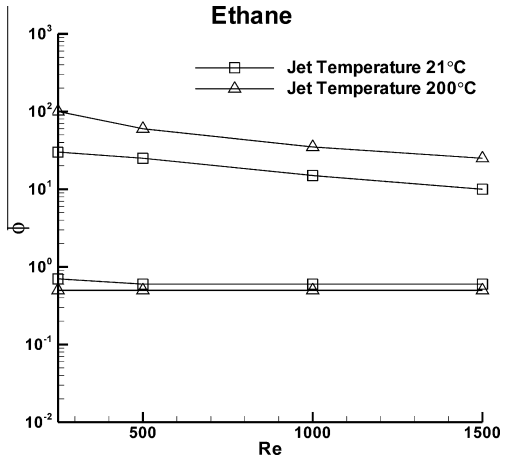

Fig. 3. Plots of φ (log scale) vs. Re showing the experimental lean and rich reactive limits of ethane/air mixtures over platinum and for different values of T_{jet}.

around the platinum plate are then presented for a range of ethane cases. The last section presents a comparison for the different fuels including a discussion of the results. Measured mole fractions are presented here on a dry-basis to remove any potential inconsistencies between the various fuels arising from deducing the water mole fractions.

3.1. Peak temperatures and reactivity limits for ethane

Fig. 2 shows the profiles of the peak plate temperature ($T_{P,max}$) vs. equivalence ratio (note the logarithmic scale) measured in ethane/air mixtures at Reynolds numbers ranging from 250 upto 1500. Three plots are shown corresponding to initial approach temperatures of 21 °C, 200 °C, and 400 °C. Note that the extent of the plots in Fig. 2 does not necessarily indicate the full reactive limits; these are shown in full and further discussed in Fig. 3. A horizontal arrow, where present, marks self-ignition of the fuel mixture on the platinum plate. The absence of an arrow indicates that ignition was forced using a blow torch as described earlier. The following observations can be made:

- Regardless of the temperature of the incoming ethane/air mixture (T_{jet}), the maximum value of the peak plate temperature occurs at moderately rich mixtures of $\varphi = 1.3$ and increases with increasing Reynolds numbers. At $T_{jet} = 21$ °C, the peak measured platinum temperature at $\varphi = 1.3$ increases from $T_{p,max} = 1310$ °C to 1340 °C as the Reynolds number increases from 250 to 500. When the Re further increases to 1000 and 1500 a flame is ignited.
- Gaps in the measured profiles shown in Fig. 2 mark the presence of flaming combustion which is disregarded here. In these cases, a gaseous flame may ignite and shroud the plate leading to extremely high temperatures. Flaming combustion occurs for ethane/air mixtures at $T_{jet} = 21$ °C and Re = 1000 and 1500 as

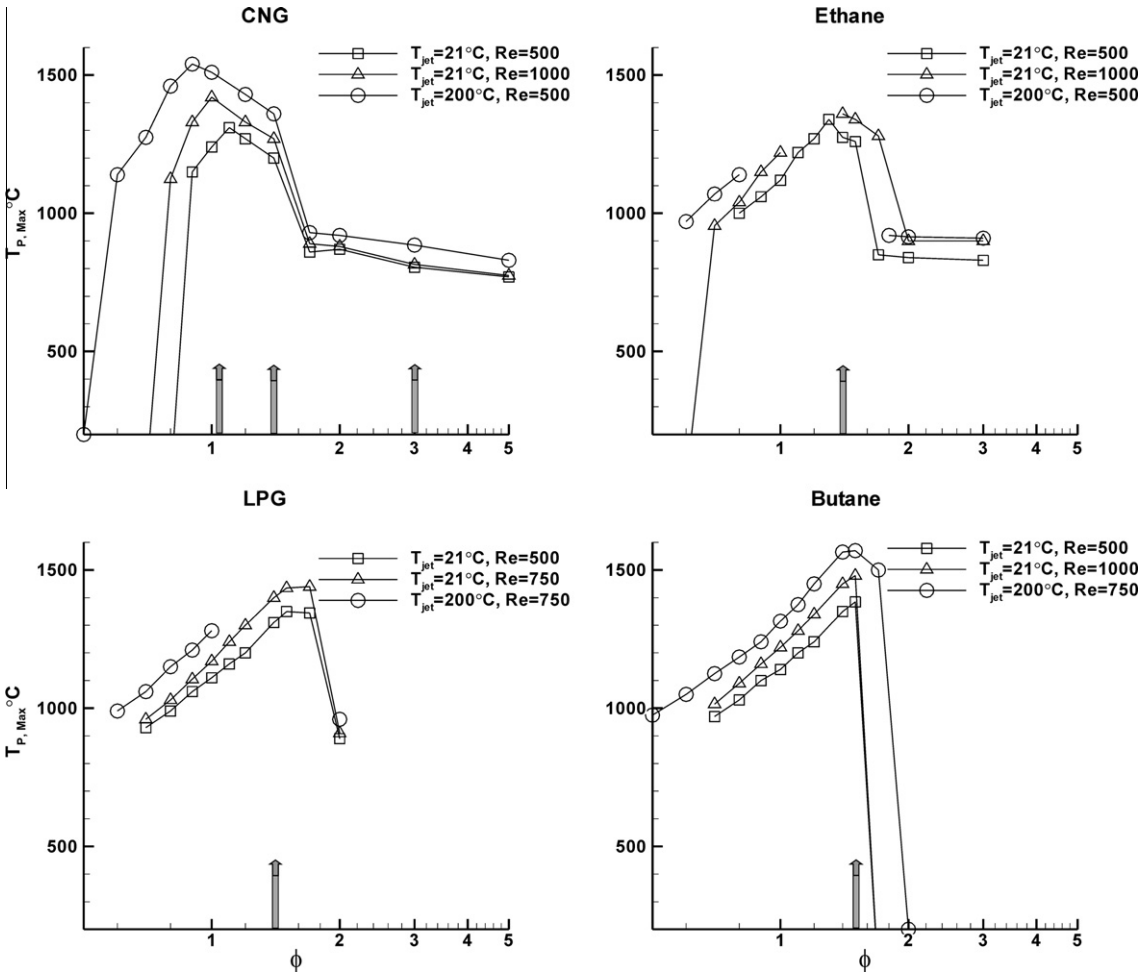

Fig. 4. $T_{P,\,max}$ vs. φ (note the logarithmic scale) for four different fuels. Vertical bars and arrows point to the equivalence ratios for species analysis.

Table 2
Flow conditions of the selected fuel/air cases for gas analysis.

Fuel	Case #	T_{jet} (°C)	Re	Velocity (m/s)	φ	He (%) in reactants
Ethane	E1	21	500	0.328	0.97	4.12
	E2	21	500	0.32	1.43	3.94
	E3	21	500	0.3	3.17	4.03
	E4	21	1000	0.648	1.44	4.6
	E5	200	500	0.76	2.47	4.4
CNG		21	500	0.346	1.41	4.32
LPG		21	500	0.31	1.45	4.13
Butane		21	500	0.328	1.52	4.16

well as for all Reynolds numbers at T_{jet} = 200 °C and 400 °C. Note that, as expected, flaming combustion occurs within the flammability limits of the gaseous mixture.

- Rich ethane/air mixtures experience a transition to extinction in two stages depending on the equivalence ratio. There is a region of fast decay in $T_{p,max}$ that extends from φ = 1.3 to an intermediately rich equivalence ratio where $T_{p,max}$ decreases to around 850 °C. This limit of $T_{p,max} \sim$ 850 °C is reached around φ = 1.7 at T_{jet} = 21 °C and Re = 250 and 500, but it increases to φ = 2 for Re = 1000 and 1500. At higher values of T_{jet}, a dependence on the Reynolds number is observed such that, at T_{jet} = 400 °C, the 900 °C limits are reached at φ = 1.7 for Re = 250 and at φ = 3.0 for Re = 1500.
- For ethane/air mixtures at T_{jet} = 400 °C, self-ignition occurs at φ > 0.4 regardless of the Reynolds numbers, as indicated by the arrow on the 400 °C plot in Fig. 2. A mixture of ethane/air at 400 °C and an equivalence ratio higher than 0.4 self-ignites on platinum and so does not need any external heat source (i.e., blow torch) to initiate the reactions. This could be of great importance in micro-burners where ignition is an issue.

The reactive limits for the ethane fuel are presented in Fig. 3 as plots of equivalence ratio vs. Reynolds number for various fuel mixture temperatures (T_{jet}). Note that the φ axis shows logarithmic scales. The lean and rich reactive limits (φ_L, φ_R) are shown for each value of T_{jet}. The reactive limits are defined as the condition when the temperature rise decreases to nearly zero, i.e. when the temperature of the platinum (or the gas downstream of it, if measured by the thermocouple) drops to that of the incoming fuel

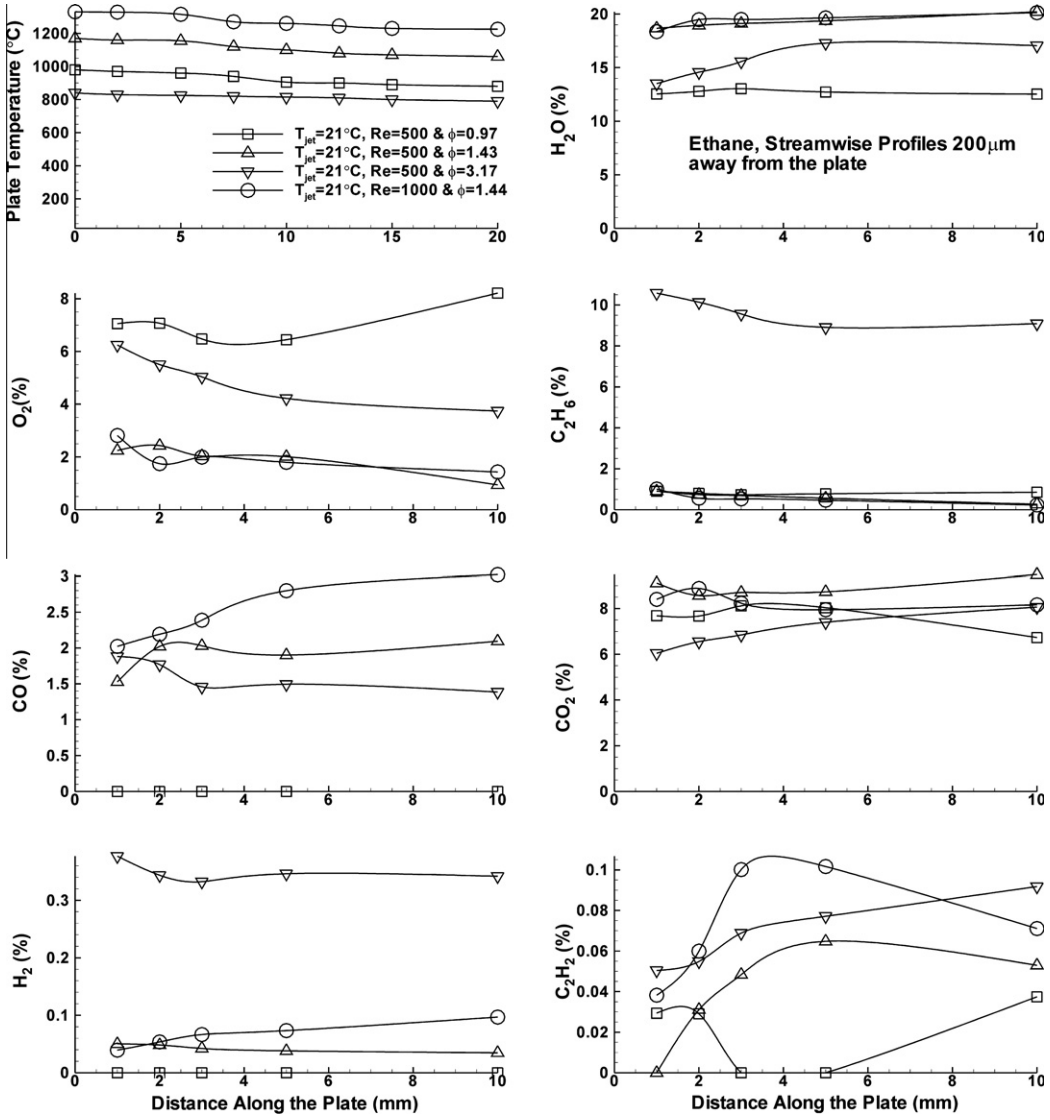

Fig. 5. Streamwise profiles of the temperature and H_2O, O_2, C_2H_6, CO, CO_2, H_2, and C_2H_2 wet-based mole fractions 200 μm away from the plate for Cases E1, E2, E3, and E4 using ethane/air mixtures.

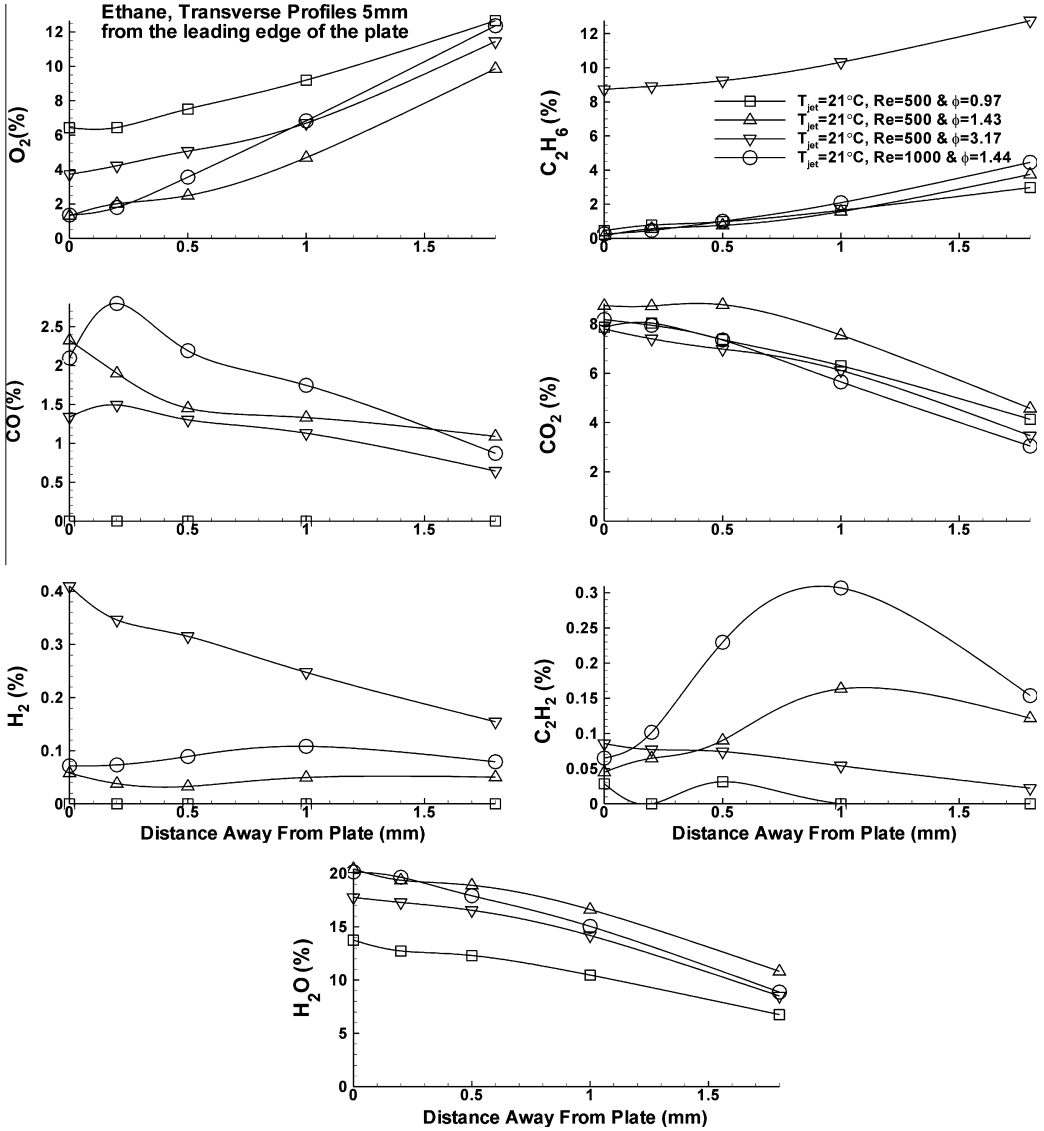

Fig. 6. Transverse profiles of O_2, C_2H_6, CO, CO_2, H_2, C_2H_2, and H_2O wet-based mole fractions 5 mm downstream of the leading edge of the plate for Cases E1, E2, E3, and E4 using ethane/air mixtures.

mixture stream. It should be noted that these limits are determined from temperature measurements obtained using either a pyrometer (for temperatures from 700 °C to 2000 °C) or a thermocouple placed on top of the platinum plate.

It is evident from Fig. 3 that ethane on platinum yields broader reactive limits than those for the gas phase alone and, depending on the flow conditions, the reactivity may extend to extreme conditions. The following additional observations are noted:

- The lean reactive limits, $\varphi_{L,}$ are generally independent of the Reynolds number and decrease with the increasing temperature of the mixture. This statement is true for gas phase mixtures and implies that gas phase chemical kinetics play a significant role in determining φ_L.
- The rich reactive limits, $\varphi_{R,}$ vary wildly between cases as shown in Fig. 3 and they are much higher than the rich limits computed for gaseous mixtures of the same fuel at similar flow conditions. For example, for an ethane/air mixture at T_{jet} = 21 °C and Re = 250, the rich gaseous flammability limits calculated using the correlation of Zabetakis [35] is 2.36 whereas, in the presence of platinum and for similar flow conditions, this limit increases to φ_R = 35. The same broadening of reactivity limits is observed at higher T_{jet} and Reynolds numbers.
- The trend observed for ethane is that φ_R increases at higher T_{jet} values regardless of the Reynolds number and it decays with increasing Re.

The corresponding reactive limits for CNG, LPG, butane and DME were reported earlier [34], and are partially reproduced in Fig. 4 for comparison with ethane. It is evident that all fuels except CNG, show a peak in the platinum plate temperature at slightly rich mixtures while the corresponding peak for CNG occurs around stoichiometric. The broadening in the rich reactive limits is highest for DME followed by CNG, ethane, LPG and then butane. Additionally, the transition to extinction is increasingly sharper for butane than for CNG, for example. This ordering may be dictated by a number of factors including sooting properties and Lewis number effects. It is worth here that the expected sooting propensity of these fuels [36] is broadly in the reverse of the rich reactive limits with butane having a higher potential that DME to produce soot. Further investigations are clearly needed to confirm the factors controlling the reactive limits of these fuels over platinum.

3.2. Product species analysis for ethane

Selected cases for species analysis are described in detail in Table 2 for all fuels studied here. Five ethane cases (E1–E5) are chosen to highlight the effects of φ, Re, and T_{jet} on the product species. Also listed in Table 2 are the approach velocities of the reactants and the helium content for the various cases. The reference Reynolds and temperature are taken as 500 and 21 °C, respectively. The vertical bars and arrows in Fig. 4 mark the location of the selected cases with respect to equivalence ratio.

Composition results presented in this section are wet-based with Figs. 5 and 6 showing respectively, streamwise and transverse profiles measured in ethane Cases E1, E2, E3, and E4 (listed in Table 2). Fig. 5 presents streamwise profiles for temperature and the wet-based mole fractions of H_2O, O_2, C_2H_6, CO, CO_2, H_2, and C_2H_2 while Fig. 6 shows the transverse profiles for the same species measured at 5 mm from the leading edge of the plate. The following observations are made with respect to the streamwise profiles shown in Fig. 5:

- Surface temperature along the plate increases when the equivalence ratio increases from 0.97 to 1.43, but then decreases significantly for an equivalence ratio of 3.17. The plate temperature also increases with Re and this is in agreement with earlier observations for ethane as well as other hydrocarbons [34]. The temperature from the leading to the trailing does decreases by around 100–150 °C for all the cases shown here.
- The main products of burning the ethane/air mixture over platinum are CO, CO_2, H_2O, and H_2. Also, C_2H_2 which is a precursor of soot, appears in the products albeit in small quantities. The peaks in the mole fractions of CO_2 and H_2O occur on the platinum surface. Peak mole fractions of around 9% for CO_2 and 20% for H_2O are obtained for the lightly rich mixture with $\varphi = 1.43$. The theoretical limit for a stoichiometric ethane/air mixture is 16.5% for water and the discrepancy is largely due to compounded error associated with the wet-based analysis. Despite this, it was felt appropriate to present the wet-based results as obtained. It should be noted that when presented

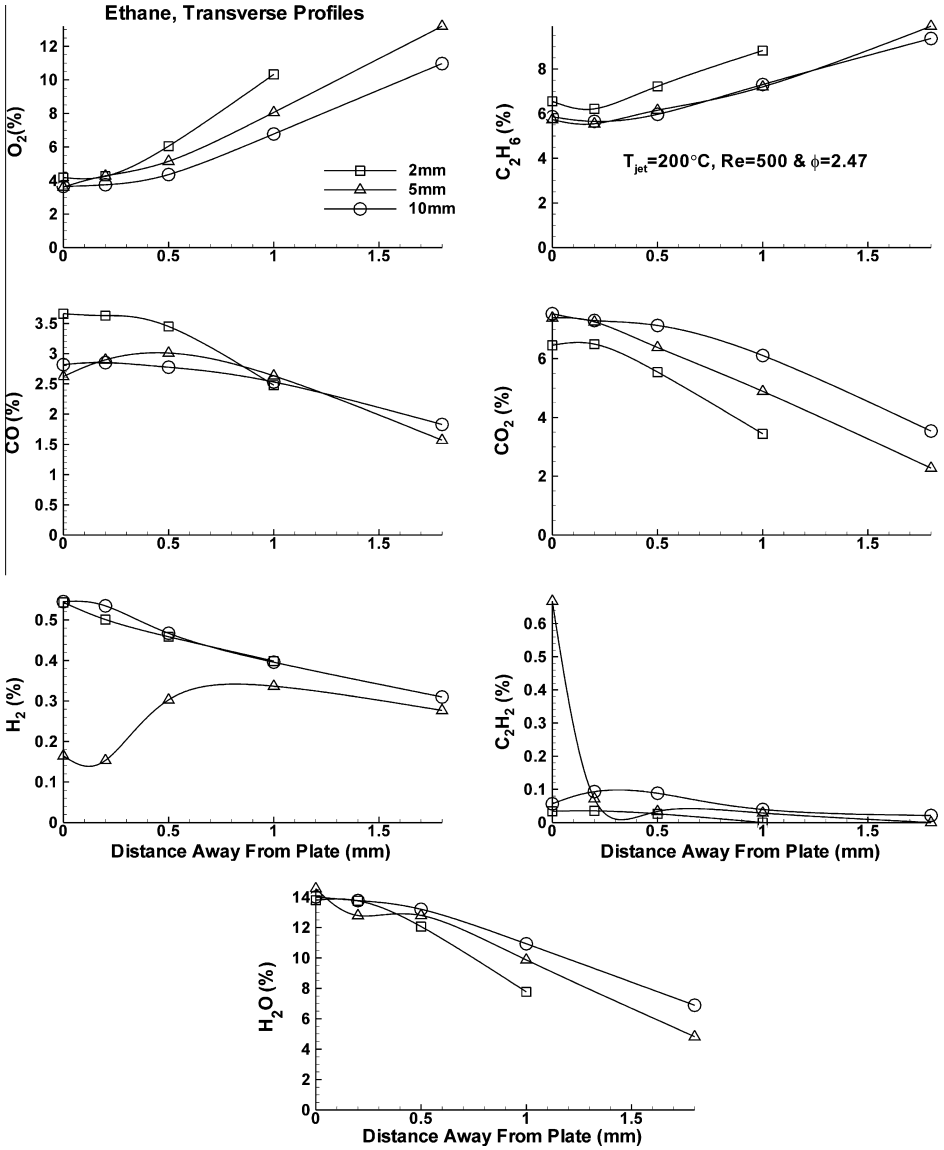

Fig. 7. Transverse profiles of O_2, C_2H_6, CO, CO_2, H_2, C_2H_2, and H_2O wet-based mole fractions 2 mm, 5 mm, and 10 mm downstream of the leading edge of the plate for Case E5 using ethane/air mixtures.

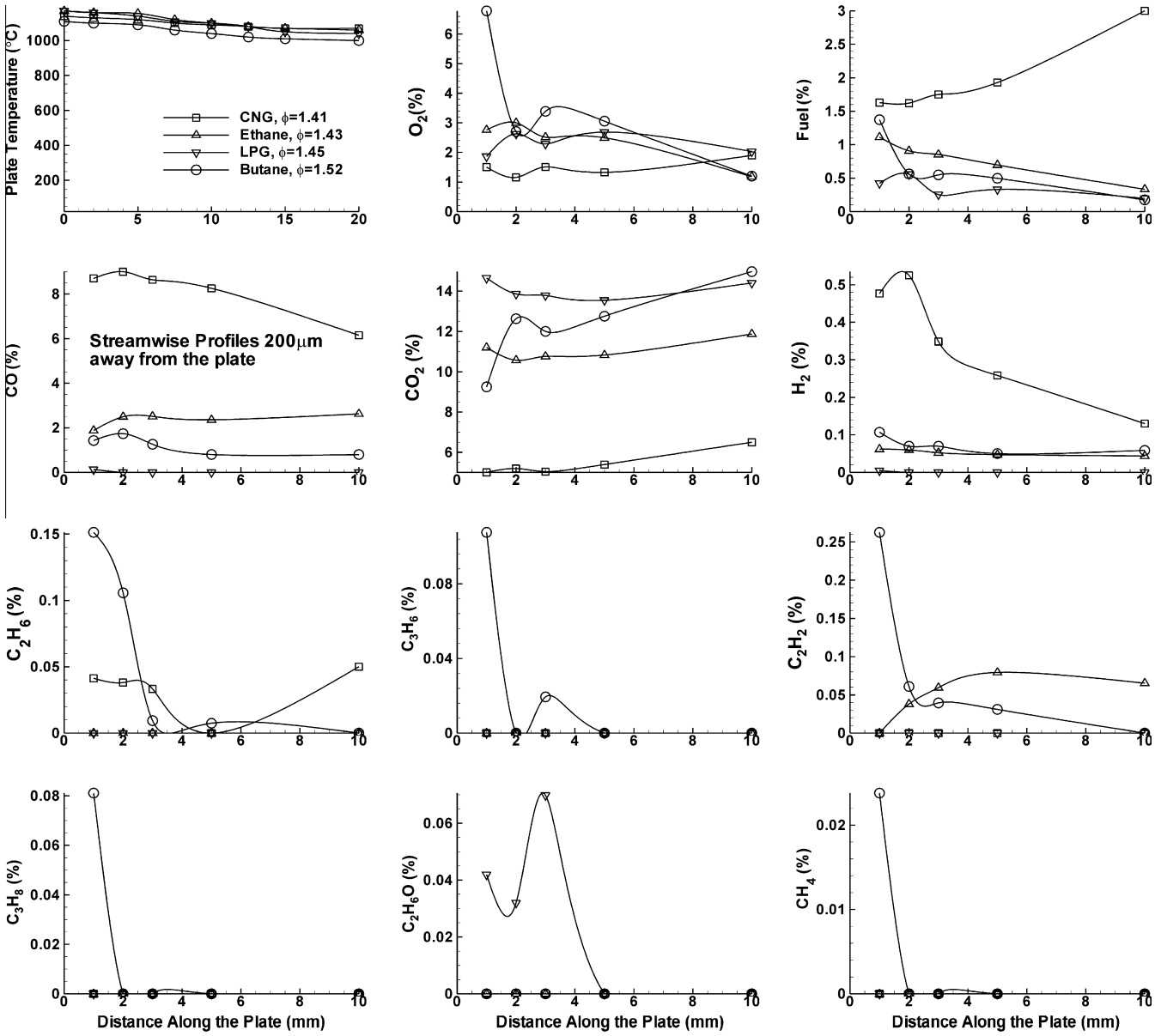

Fig. 8. Streamwise profiles of temperature, O_2, fuel, CO, CO_2, H_2, C_2H_6, C_3H_6, C_2H_2, C_3H_8, C_2H_6O, and CH_4 dry-based mole fractions 200 μm away from the plate for various fuel/air mixtures.

on a dry-basis (not shown here), the trends obtained are identical and the peak mole fractions of CO_2 increases from 9% to about 11%.

- Acetylene mole fractions, albeit low, increase when φ increases from 0.97 to 3.17 and this is expected for such rich mixtures. Hydrogen does not appear in the products for the lean case and exists in low quantities (0.05%) for Case E2 (φ = 1.43) but increases significantly at φ = 3.17.
- In the streamwise direction, the plate can be divided nominally into two zones: (i) the leading edge zone which extends from 0 mm to 5 mm from the leading edge and (ii) the trailing zone which covers the rest of the plate (5–10 mm). The distribution of species within these zones is different. Oxygen and fuel decay when moving away from the leading edge before stabilizing at around 5 mm. Product species such as CO, CO_2, H_2O, and H_2 show gradients in the leading edge zone but stabilize further downstream.
- Oxygen at the plate decreases as the equivalence ratio increases from 0.97 to 1.43. This is largely due to preferential thermal diffusion which favors oxygen more than ethane and results in leaner mixtures near the plate so that the nominal case E2 with φ = 1.43 in the free stream will be closer to a stoichiometric mixture near the plate. For the very rich mixture with φ = 3.17, oxygen is still present near the plate (~4%) implying that the surface may have been saturated. This competition between species driven by their sticking coefficients as well as differential diffusion is an interesting and complex process that warrants further studies.

The transverse profiles shown in Fig. 6 confirm most of the above findings and the following observations may be added:

- Carbon monoxide peaks away from the plate for φ = 3.17, while hydrogen and CO_2 peak away from the plate for φ = 1.43. The peak in product species away from the plate is most likely due to gaseous reactions. This is also true for acetylene which also peaks away from the plate for most conditions shown in Fig. 6.

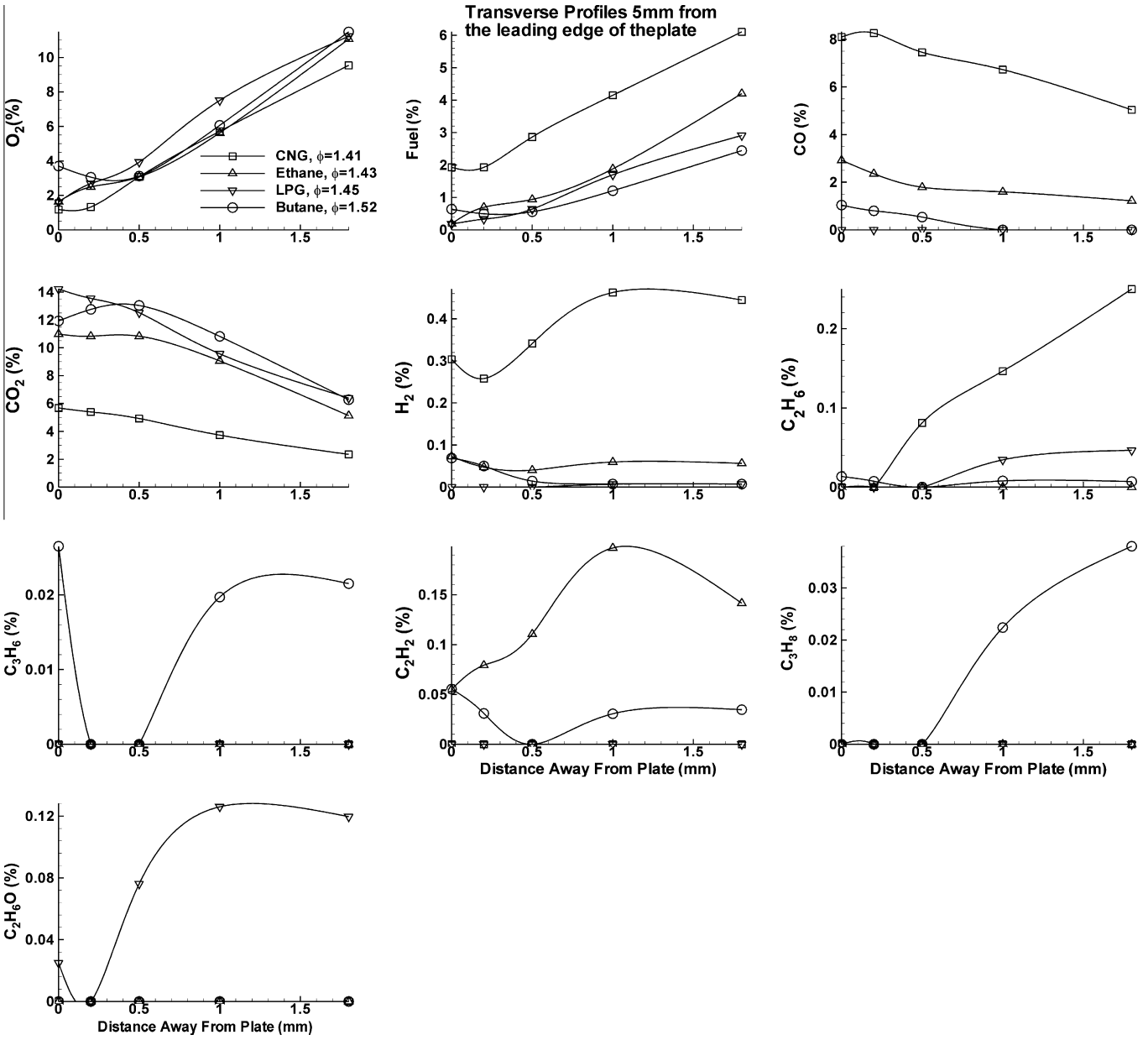

Fig. 9. Transverse profiles of O_2, fuel, CO, CO_2, H_2, C_2H_6, C_2H_2, C_3H_6, C_2H_2, C_3H_8, and C_2H_6O dry-based mole fractions 5 mm downstream of the leading edge for various fuel/air mixtures.

- The boundary layer may be nominally divided in two regions: (i) an inner layer adjacent to the plate where surface reactions dominate and (ii) an outer layer where gaseous reactions play a more dominant role. This issue is further examined in a later section of this paper.
- Transverse profiles of species mole fractions measured at 2 mm, 5 mm, and 10 mm from the leading edge of the plate for Case E5 are shown in Fig. 7. The following observations are made:
- Oxygen and C_2H_6 experience a leading edge effect where they decrease as they move away from the leading edge after stabilizing 5 mm from the leading edge.
- Carbon monoxide and hydrogen exist in higher percentages (3% and 0.5%, by volume, respectively) for Case E5 than the other four cases. The leading edge effect is reflected in the CO distribution where it is formed in higher quantities near the leading edge of the plate and decays further downstream.
- Acetylene peaks near the plate for the three transverse locations (2 mm, 5 mm, and 10 mm), then it decays as it moves further away from the plate.

3.3. Comparison between fuels and discussion

A comparison is made here for the temperature and species mole fractions measured in the four fuels tested in this paper. Cases selected for comparison have the same Reynolds number (Re = 500) and jet temperature T_{jet} = 21 °C with equivalence ratios that are as close as possible and ranging from 1.41 to 1.52. Further details about these cases are shown in Table 2. Temperature and the mole fractions of O_2, fuel, CO, CO_2, H_2, C_2H_6, C_3H_6, C_2H_2, C_3H_8, and C_2H_6O (DME) are presented in Fig. 8 for the streamwise direction and in Fig. 9 for the transverse profiles at 5 mm from the leading edge. Results are presented here on a dry-basis to remove any

potential error in the comparison resulting from the wet-based analysis that is subject to thermal diffusion effects which may be different for different fuels. The following observations can be made:

- The surface temperature on the plate is similar for all fuels and so is the overall structure relayed from the measured species profiles in that two zones, leading edge zone and a trailing zone are observed along the plate. In the transverse direction, an inner layer closer to the plate as well as an outer layer further away are noted for all fuels.
- The extent of differential thermal diffusion may be crudely related to ratio of oxygen over fuel measured near the plate for the different fuels. If we disregard the slight differences in equivalence ratios and assume the same oxygen/fuel in the free stream, then in the absence of differential diffusion, this ratio should be the same near the plate. It is evident from the plots shown in Figs. 8 and 9 that the oxygen/fuel ratio near the platinum is lowest for CNG and increases for the heavier fuels. This correlates well with the relative molecular weights and the expected thermal diffusion of the species.
- The measured mole fractions of CO_2 are consistent at least in trend with those expected from the stoichiometric decomposition of the fuels with CNG < ethane < butane < LPG. The absolute mole fractions differ however due to the relative selectivity for CO compared to CO_2. It is clear from both the streamwise and transverse profiles that the selectivity for CO is highest for CNG followed by ethane, butane, and then LPG. This trend is also reflected for hydrogen with the highest selectively being for CNG and the lowest for LPG.
- Products such as C_2H_6, C_2H_2, C_3H_6, CH_4, and C_3H_8 are detected when burning butane/air mixtures, while DME is only detected near the leading edge of the plate when burning the LPG/air mixture over platinum.
- Carbon dioxide decays away from the plate for all fuels except butane where it peaks 0.5 mm away from the plate. Carbon monoxide decays away from the plate for all fuels except CNG where it experiences a local maximum in the vicinity of the plate. H_2 behaves similarly to CO, but its peak is further away from the plate which is indicative of gaseous reactions coming into effect.

Compositions on a wet-basis (not shown here) yield similar trends to those shown here for the dry-basis measurements hence confirming that the conclusions are not affected by errors from the wet analysis. It is also worth noting that the compositions reported here, particularly at the leading edge of the plate are consistent with those recently reported by Smyth and Kyritsis [20] who also reported flowfield measurements in the vicinity of the plate Two issues warrant further studies, namely the extent of differential thermal diffusion for the various fuels and the varying selectivities with respect to CO/CO_2 and H_2/H_2O conversion. Numerical studies may assist significantly in quantifying the former issue while the issue of selectivity requires the knowledge of detailed surface mechanisms that adequately represent the heterogeneous chemistry of the fuel on platinum. Such mechanisms exist for methane but need to be developed for the remaining fuels.

4. Conclusions

Measurements of surface temperature and species mole fractions are made to study the reactivity of platinum with four hydrocarbon fuels (compressed natural gas, liquefied petroleum gas, butane, and ethane). The effects of the jet temperature (T_{jet}), equivalence ratio (φ), and the Reynolds number of the issuing gas (Re) on the reactivity of these hydrocarbons on platinum are investigated. The main conclusions from this study are listed here:

- The reactive limits of ethane/air mixtures broaden significantly in the presence of platinum compared to the gaseous flammability limits. The temperature of the plate increases with increasing Re and T_{jet} and peaks at moderately rich ethane/air mixtures ($\varphi = 1.3$) before transitioning to a low temperature for richer mixtures ($\varphi = 1.7–2$).
- The main products of reaction over platinum for the four alkanes are CO_2 and H_2O while CNG showing the highest selectivity to CO and H_2. A range of hydrocarbon products are measured in small quantities when burning butane and LPG/air mixtures over platinum.
- Streamwise to the plate, two nominal reactive zones are identified as a leading edge zone extending for the first 5 mm or so and a trailing zone covering the rest of the plate. In the transverse direction, an inner layer is noted near the plate and an outer layer where gaseous reaction may occur.
- The oxygen to fuel ratio near the plate is different than that injected in the free stream and this is mostly caused by differential thermal diffusion. Heavier alkanes such a butane and propane results in the largest differential and hence a leaner mixture near the plate than that originally injected.

Acknowledgment

This research is supported by the Australian Research Council.

References

[1] Fernandez-Pello C. Micropower generation using combustion: issues and approaches. Proc Combust Inst 2002;29:883–99.
[2] Dunn-Rankin D, Leal E, Walther D. Personal power systems. Prog Energy Combust Sci 2005;31:422–65.
[3] Maruta K. Micro and mesoscale combustion. Proc Combust Inst 2011;33:125–50.
[4] Ju Y, Maruta K. Microscale combustion: technology development and fundamental research. Prog Energy Combust Sci 2011;37:669–715.
[5] Weinberg FJ, Rowe DM, Min G, Ronney PD. On thermoelectric power conversion from heat recirculating combustion systems. Proc Combust Inst 2002;29:941–7.
[6] Kolb G, Schürer J, Tiemann D, Wichert M, Zapf R, Hessel V, et al. Fuel processing in integrated micro-structured heat-exchanger reactors. J Power Sources 2007;171:198–204.
[7] Mei H, Li C, Ji S, Liu H. Modeling of a metal monolith catalytic reactor for methane steam reforming-combustion coupling. Chem Eng Sci 2007;62:4294–303.
[8] Hickman DA, Schmidt LD. Steps in CH_4 oxidation on Pt and Rh surfaces: high temperature reactor simulations. AIChE J 1993;39:1164–77.
[9] Hickman DA, Schmidt LD. Production of syngas by direct catalytic-oxidation of methane. Science 1993;259:343–6.
[10] Reinke M, Mantzaras J, Schaeren R, Bombach R, Inauen A, Schenker S. Homogeneous ignition of CH_4/air and H_2O and CO_2-diluted CH_4/O_2 mixtures over Pt; an experimental and numerical investigation at pressures up to 16 bar. Proc Combust Inst 2005;30:2519–27.
[11] Appel C, Mantzaras J, Schaeren R, Bombach R, Inauen A, Kaeppeli B, et al. An experimental and numerical investigation of homogeneous ignition in catalytically stabilized combustion of hydrogen/air mixtures over platinum. Combust Flame 2002;128:340–68.
[12] Dogwiler U, Benz P, Mantzaras J. Two-dimensional modelling for catalytically stabilized combustion of a lean methane–air mixture with elementary homogeneous and heterogeneous chemical reactions. Combust Flame 1999;119:455–72.
[13] Miesse CM, Masel RI, Jensen CD, Shannon MA, Short M. Submillimeter-scale combustion. AIChE J 2004;50:3206–14.
[14] Miesse C, Masel R, Short M, Shannon M. Experimental observations of methane–oxygen diffusion flame structure in a sub-millimetre microburner. Combust Theor Model 2005;9:77–92.
[15] Chao Y-C, Chen G-B, Hsu C-J, Leu T-S, Wu C-Y, Cheng T-S. Operational characteristics of catalytic combustion in a platinum microtube. Combust Sci Technol 2004;176:1755–77.
[16] Prakash S, Glumac NG, Shankar N, Shannon MA. OH concentration profiles over alumina quartz, and platinum surfaces using laser-induced fluorescence spectroscopy in low-pressure hydrogen/oxygen flames. Combust Sci Technol 2005;177:793–817.

[17] Hwang CH, Lee CE, Lee KO. Numerical investigation on combustion characteristics of methane in a hybrid catalytic combustor. Fuel 2004;83:987–96.
[18] Evans CJ, Kyritsis DC. Operational regimes of rich methane and propane/oxygen flames in mesoscale non-adiabatic ducts. Proc Combust Inst 2009;32:3107–14.
[19] Smyth SA, Christensen KT, Kyritsis DC. Intermediate Reynolds number flat plate boundary layer flows over catalytic surfaces for micro-combustion applications. Proc Combust Inst 2009;32:3035–42.
[20] Smyth SA, Kyritsis DC. Experimental determination of the structure of catalytic micro-combustion flows over small-scale flat plates for methane and propane fuel. Combust Flame 2012;159:802–16.
[21] Karagiannidis S, Mantzaras J, Bombach R, Schenker S, Boulouchos K. Experimental and numerical investigation of the hetero-/homogeneous combustion of lean propane/air mixtures over platinum. Proc Combust Inst 2009;32:1947–55.
[22] Karagiannidis S, Mantzaras J, Boulouchos K. Stability of hetro-/homogeneous combustion in propane-and methane-fueled catalytic microreactors: channel confinement and molecular transport effects. Proc Combust Inst 2011;33:3241–9.
[23] Stefandis GD, Vlachos DG. Controlling homogeneous chemistry in homogeneous-heterogeneous reactors: application to propane combustion. Ind Eng Chem Res 2009;48:5962–8.
[24] Mantzaras J, Bombach R, Schaeren R. Hetero-/homogeneous combustion of hydrogen/air mixtures over platinum at pressures up to 10 bar. Proc Combus Inst 2009;32:1937–45.
[25] Karagiannidis S, Mantzaras J, Jackson G, Boulouchos K. Hetero-/homogeneous combustion and stability maps in methane-fueled catalytic microreactors. Proc Combust Inst 2007;31:3309–17.
[26] Reinke M, Mantzaras J, Bombach R, Schenker S, Inauen A. Gas phase chemistry in catalytic combustion of methane/air mixtures over platinum at pressures of 1–16 bar. Combust Flame 2005;141:448–68.
[27] Reinke M, Mantzaras J, Schaeren R, Bombach R, Kreutner W, Inauen A. Homogeneous ignition in high-pressure combustion of methane/air over platinum: comparison of measurements and detailed numerical predictions. Proc Combust Inst 2002;29:1021–9.
[28] Ghermay Y, Mantzaras J, Bombach R. Experimental and numerical investigation of hetro–/homogeneous combustion of $CO/H_2/O_2/N_2$ mixtures over platinum at pressures upto 5 bar. Proc Combust Inst 2011;33:1827–35.
[29] Heatwole S, Veeraragavan A, Cadou CP, Buckley SG. In situ species and temperature measurements in a millimeter-scale combustor. Nanoscale Microscale Therm Eng 2009;13:54–76.
[30] Volchko SJ, Sung CJ, Huang Y, Schneider SJ. Catalytic combustion of rich methane/oxygen mixtures for micropropulsion applications. J Propul Power 2006;22:684–93.
[31] Spadaccini CM, Zhang X, Cadou CP, Miki N, Waitz IA. Preliminary development of a hydrocarbon-fueled catalytic micro-combustor. Sensor Actuat A: Phys 2003;103:219–24.
[32] Kim NI, Kato S, Kataoka T, Yokomori T, Maruyama S, Fujimori T, et al. Flame stabilization and emission of small Swiss-roll combustors as heaters. Combust Flame 2005;141:229–40.
[33] Ahn J, Eastwood C, Stizki L, Ronney PD. Gas-phase and catalytic combustion in heat-recirculating burners. Proc Combust Inst 2005;30:2463–72.
[34] Badra JA, Masri AR. Catalytic combustion of selected hydrocarbon fuels on platinum: reactivity and hetero–homogeneous interactions. Combust Flame 2012;159:817–31.
[35] Zabetakis MG. Flammability characteristics of combustible gases and vapors. Alaska: Bureau of Mines; 1965.
[36] Calcote HF, Manos DM. Effect of molecular structure on incipient soot formation. Combust Flame 1983;49:289–304.